

Enhancing thermoelectric efficiency of GeTe through process improvement assisted by active learning and Bayesian optimization

Florent Pawula,^{*,†,‡,¶} Agathe Bajan,[†] Mathias Hamitouche,^{§,‡} Linda Abbassi,^{§,‡}
Cédric Bourgès,[§] Takao Mori,[§] Jean-François Halet,^{‡,||} David Berthebaud,^{‡,¶} and
Guillaume Lambard^{*,†,‡}

[†]*Data-driven materials design group, Center for Basic Research on Materials (CBRM),
National Institute for Materials Science (NIMS), Namiki 1-1, Tsukuba, Ibaraki, 305-0044,
Japan*

[‡]*CNRS-Saint Gobain-NIMS, IRL 3629, Laboratory for Innovative Key Materials and
Structures (LINK), National Institute for Materials Science (NIMS), Namiki 1-1, Tsukuba,
Ibaraki, 305-0044, Japan*

[¶]*Nantes Université, CNRS, Institut des Matériaux de Nantes Jean Rouxel, IMN, F-44000
Nantes, France*

[§]*Thermal Energy Group, WPI International Center for Materials Nanoarchitectonics
(WPI-MANA), National Institute for Materials Science (NIMS), Tsukuba, Japan*

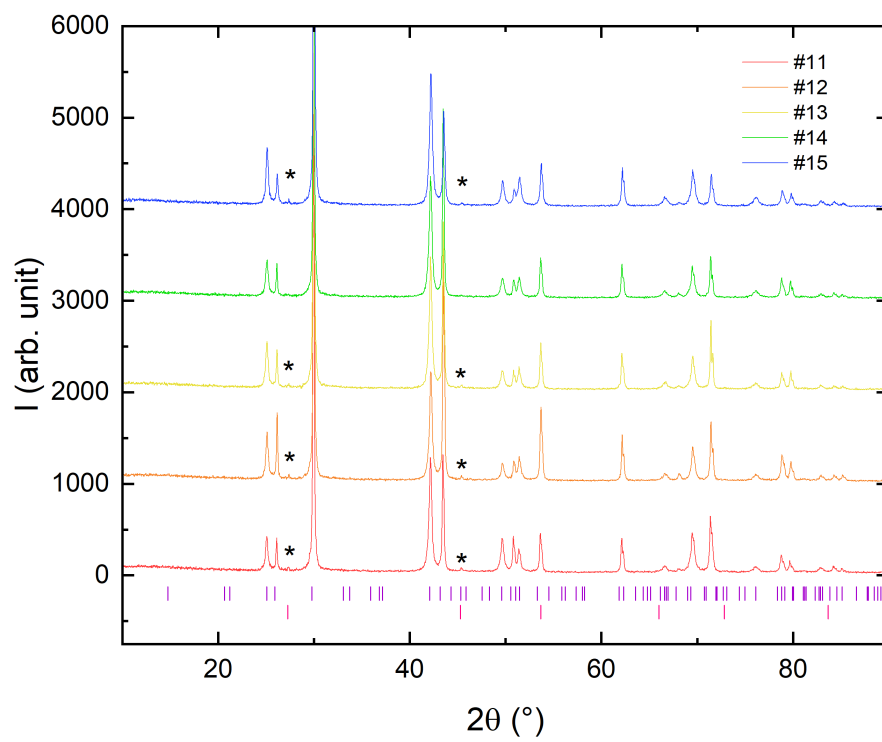
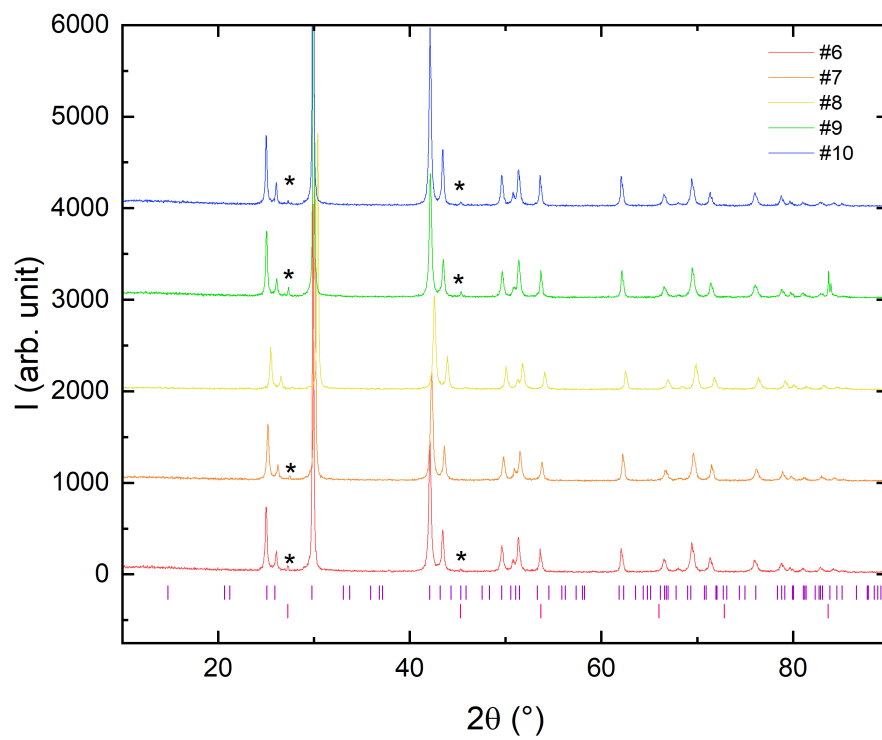
^{||}*Univ Rennes, CNRS, Ecole Nationale Supérieure de Chimie de Rennes (ENSCR), Institut
des Sciences Chimiques de Rennes (ISCR), UMR 6226, F-35000, Rennes, France*

E-mail: florent.pawula@cnrs-imn.fr; LAMBARD.Guillaume@nims.go.jp

Supplementary information

Table S1: Process parameters of the samples.

| Sample# | heating.rate (K.h ⁻¹) | T_annealing (K) | t_duration (h) | cooling.rate (K.h ⁻¹) | mass_powder (g) | milling.time.1 (min) | heating.rate.1 (K.min ⁻¹) | T_annealing.1 (K) | t_duration.1 (min) | cooling.rate.1 (K.min ⁻¹) | Uniaxial pressure (MPa) |
|---------|--------------------------------------|--------------------|-------------------|--------------------------------------|--------------------|-------------------------|--|----------------------|-----------------------|--|----------------------------|
| 0 | 25 | 1123 | 16 | 175 | 4.25 | 1 | 25 | 850 | 40 | 150 | 70 |
| 1 | 50 | 1323 | 16 | 75 | 5.75 | 1 | 100 | 800 | 20 | 175 | 40 |
| 2 | 50 | 1273 | 12 | 175 | 4.5 | 1 | 75 | 900 | 55 | 50 | 60 |
| 3 | 50 | 1073 | 12 | 50 | 5.25 | 1 | 50 | 750 | 30 | 75 | 50 |
| 4 | 115.625 | 1223 | 12 | 154.16667 | 6.7 | 15 | 75.33 | 750 | 5 | 75.33 | 60 |
| 5 | 25 | 1273 | 24 | 25 | 5.1982 | 10 | 50 | 900 | 30 | 25 | 40 |
| 6 | 25 | 1323 | 14 | 75 | 5.8184 | 6 | 150 | 750 | 15 | 75 | 50 |
| 7 | 75 | 1423 | 18 | 25 | 5.9029 | 9 | 50 | 938 | 0 | 140 | 40 |
| 8 | 50 | 1473 | 22 | 75 | 5.1522 | 6 | 200 | 850 | 35 | 200 | 50 |
| 9 | 75 | 1423 | 24 | 50 | 5.2986 | 4 | 175 | 850 | 25 | 25 | 50 |
| 10 | 10.5 | 1348 | 24 | 75 | 4.52333 | 2 | 201 | 700 | 25 | 48 | 40 |
| 11 | 30 | 1348 | 24 | 75 | 5.5103 | 8 | 138 | 850 | 25 | 139 | 45 |
| 12 | 10.5 | 1448 | 0.1 | 75 | 4.52489 | 2 | 167 | 800 | 25 | 123 | 40 |
| 13 | 30 | 1123 | 16 | 25 | 6.05351 | 4 | 151 | 750 | 25 | 47 | 50 |
| 14 | 20 | 1348 | 24 | 50 | 5.75132 | 6 | 96 | 875 | 15 | 100 | 55 |
| 15 | 52.4 | 1348 | 18 | 25 | 4.61276 | 9 | 27.2 | 900 | 25 | 105.4 | 60 |
| 16 | 125 | 1373 | 6 | 100 | 4.10237 | 5 | 184 | 800 | 15 | 47.4 | 60 |
| 17 | 113.9 | 1273 | 22 | 25 | 5.19576 | 15 | 138 | 800 | 10 | 106.8 | 55 |
| 18 | 97.5 | 1223 | 6 | 77.3 | 3.74733 | 13 | 113 | 700 | 10 | 109 | 50 |
| 19 | 32 | 1273 | 22 | 25 | 4.12751 | 3 | 27.4 | 850 | 25 | 159 | 65 |
| 20 | 120 | 1098 | 22 | 75 | 5.252 | 3 | 125 | 750 | 5 | 175 | 45 |
| 21 | 10 | 1448 | 2 | 100 | 4.505 | 12 | 150 | 850 | 10 | 100 | 55 |
| 22 | 80 | 1398 | 22 | 100 | 5.752 | 3 | 125 | 900 | 0 | 50 | 50 |
| 23 | 130 | 1023 | 6 | 100 | 5.25 | 11 | 175 | 900 | 5 | 125 | 40 |



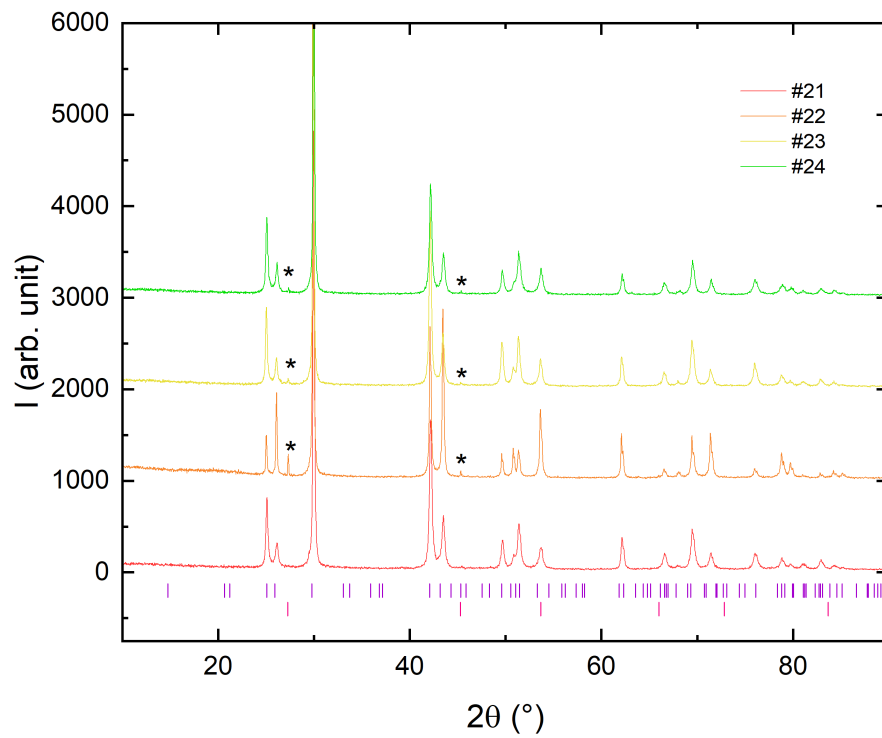
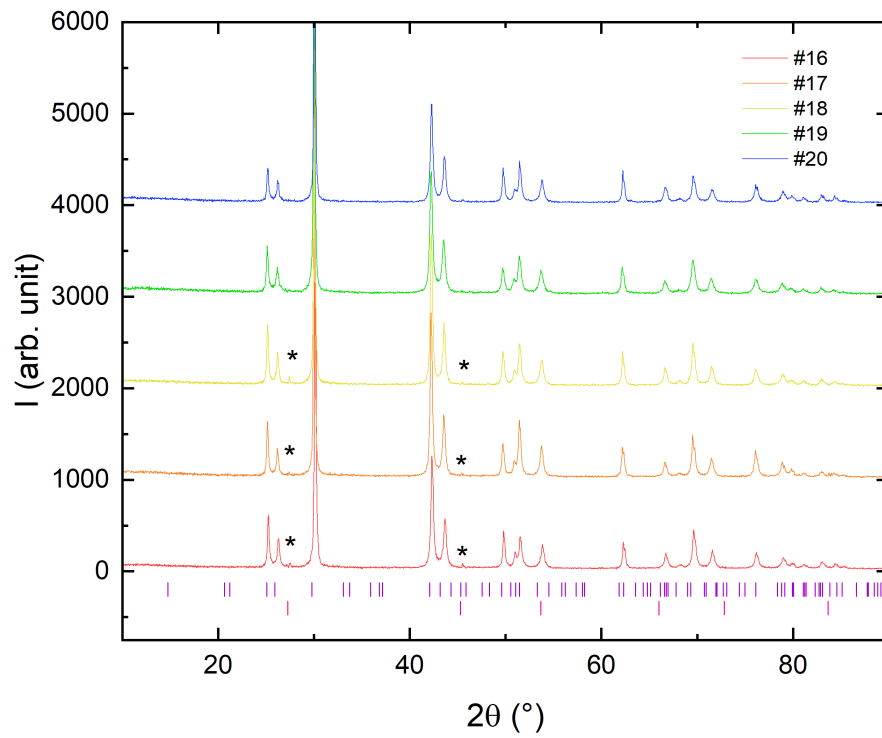


Figure S1: X-ray diffraction patterns associated with the Bragg peak positions of trigonal GeTe ($R\bar{3}m$) and cubic Ge ($Fd\bar{3}m$). The * denotes the presence of elemental Ge.

Table S2: Le Bail refinement parameters extracted from XRD patterns.

| Sample | a (Å) | (a) (Å) | c (Å) | (c) (Å) | $\langle d \rangle$ (Å) | $\langle\langle d \rangle\rangle$ (Å) | Chi ² | R_Bragg | R_F |
|--------|---------|---------|----------|---------|-------------------------|---------------------------------------|------------------|---------|-------|
| 0 | 8.32898 | 7E-5 | 10.67244 | 1.3E-4 | 755.81 | 0.87 | 2.45 | 1.8 | 3.31 |
| 1 | 8.3309 | 1.6E-4 | 10.6736 | 2.7E-4 | 637.31 | 0.05 | 3.47 | 2.38 | 3.73 |
| 2 | 8.33097 | 7E-5 | 10.66495 | 1.8E-4 | 750.39 | 0.05 | 2.83 | 4.65 | 10.52 |
| 3 | 8.32922 | 9E-5 | 10.6701 | 2.1E-4 | 550.67 | 0.57 | 3.18 | 2.73 | 5.2 |
| 4 | 8.33326 | 6E-5 | 10.6763 | 2E-4 | 305.8 | 0.25 | 3.69 | 2.03 | 5.68 |
| 5 | 8.32907 | 1.2E-4 | 10.67576 | 1.6E-4 | 488.49 | 0.33 | 2.36 | 5.52 | 10.02 |
| 6 | 8.33442 | 1.8E-4 | 10.67958 | 2.6E-4 | 412.33 | 0.28 | 1.69 | 1.66 | 2.43 |
| 7 | 8.33812 | 1.3E-4 | 10.69258 | 1.8E-4 | 471.05 | 0.68 | 2.03 | 2.32 | 6.2 |
| 8 | 8.32745 | 1E-4 | 10.67811 | 1.6E-4 | 524.09 | 0.53 | 2.59 | 1.51 | 2.71 |
| 9 | 8.33116 | 8E-5 | 10.67306 | 1.5E-4 | 569.24 | 0.59 | 2.23 | 1.15 | 2.45 |
| 10 | 8.33295 | 9E-5 | 10.67242 | 2.2E-4 | 520.25 | 0.1 | 3.46 | 2.65 | 5.35 |
| 11 | 8.32997 | 8E-5 | 10.67417 | 1.9E-4 | 692.56 | 0.92 | 4.32 | 1.68 | 4.63 |
| 12 | 8.33044 | 9E-5 | 10.67576 | 2.1E-4 | 596.8 | 0.66 | 4.43 | 1.73 | 4.06 |
| 13 | 8.33358 | 9E-5 | 10.67232 | 2.2E-4 | 538.64 | 0.25 | 3.94 | 1.96 | 3.34 |
| 14 | 8.32923 | 1.1E-4 | 10.68117 | 2E-4 | 511.68 | 0.48 | 3.75 | 1.58 | 4.31 |
| 15 | 8.33184 | 1.1E-4 | 10.68418 | 1.8E-4 | 431.48 | 0.12 | 2.54 | 1.45 | 4.52 |
| 16 | 8.33128 | 1E-4 | 10.67865 | 1.6E-4 | 491.05 | 0.48 | 2.79 | 4.25 | 7.61 |
| 17 | 8.3315 | 1.1E-4 | 10.6801 | 1.8E-4 | 474.62 | 0.18 | 2.98 | 1.87 | 4.37 |
| 18 | 8.33429 | 1.4E-4 | 10.67578 | 2.4E-4 | 357.57 | 0.44 | 3.15 | 2.02 | 7.07 |
| 19 | 8.33074 | 1.2E-4 | 10.68204 | 1.8E-4 | 474.67 | 0.43 | 2.66 | 1.34 | 2.43 |
| 20 | 8.3337 | 1.3E-4 | 10.68167 | 1.9E-4 | 411.69 | 0.61 | 3.07 | 2.84 | 6.18 |
| 21 | 8.32752 | 6E-5 | 10.67397 | 1.4E-4 | 898.95 | 0.56 | 3.02 | 1.65 | 2.71 |
| 22 | 8.33156 | 9E-5 | 10.67583 | 1.6E-4 | 451.86 | 0.65 | 2.6 | 1.71 | 4.48 |
| 23 | 8.32592 | 1.3E-4 | 10.67917 | 2E-4 | 413.46 | 0.56 | 3.16 | 2.58 | 5.79 |

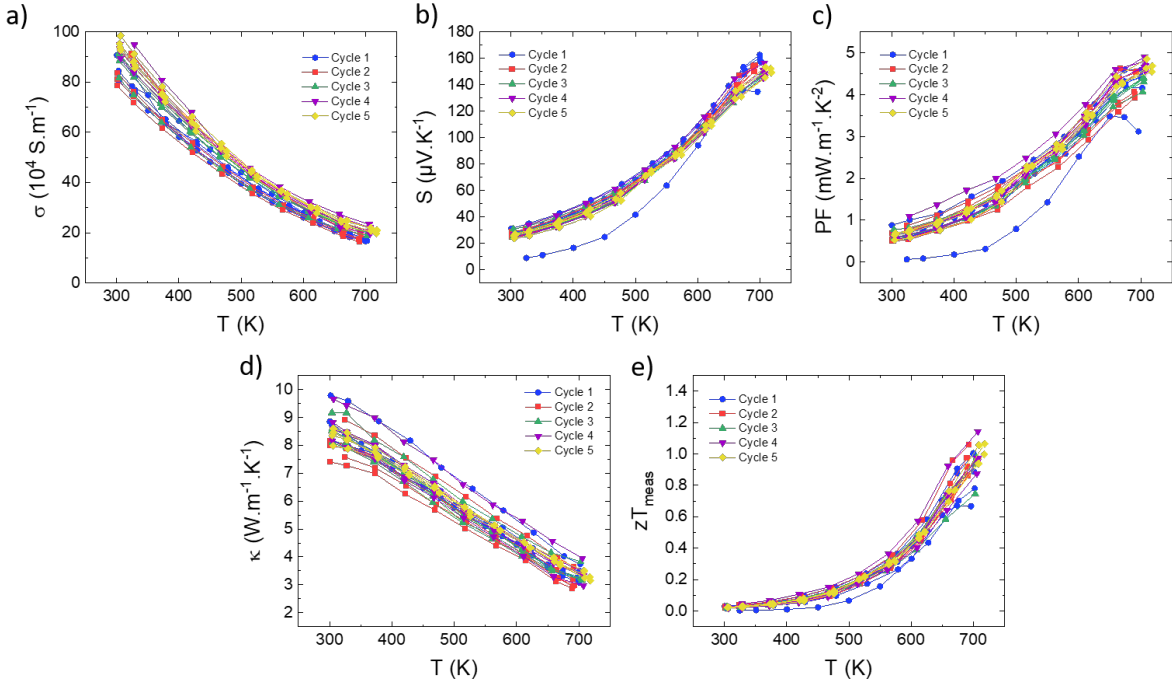


Figure S2: Thermoelectric properties of the samples as a function of temperature from cycle 1 to cycle 5. Electrical conductivity (a), Seebeck coefficient (b), power factor (c), thermal conductivity (d), and figure of merit (e).

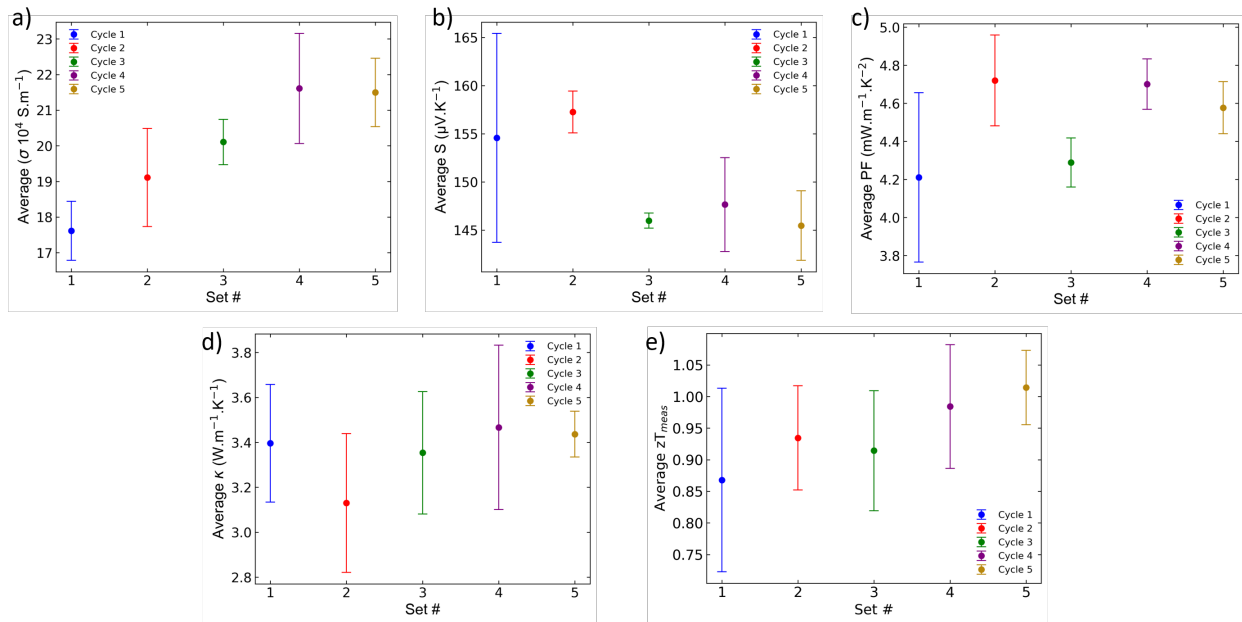


Figure S3: Average of the thermoelectric properties at 700 K as a function of sample number from cycle 1 to cycle 5. Electrical conductivity (a), Seebeck coefficient (b), power factor (c), thermal conductivity (d), and figure of merit (e).

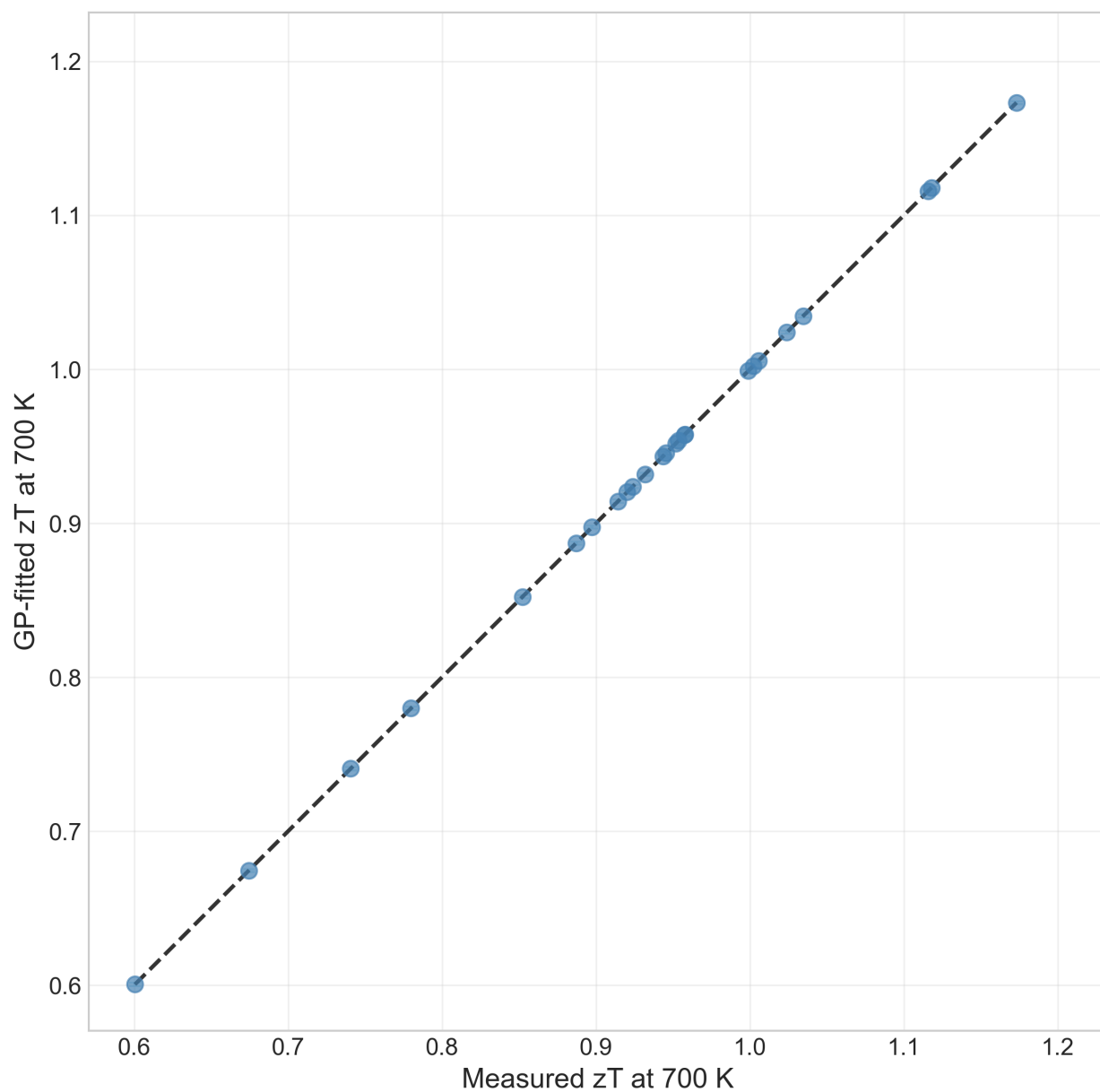


Figure S4: GP-fitted zT at 700 K as a function of measured zT at 700 K for all 25 GeTe samples. The perfect prediction line is shown in black. The error bars, large of 0.001 in average and therefore not visible, represent a single standard deviation of the GP-fitted zT at 700 K.

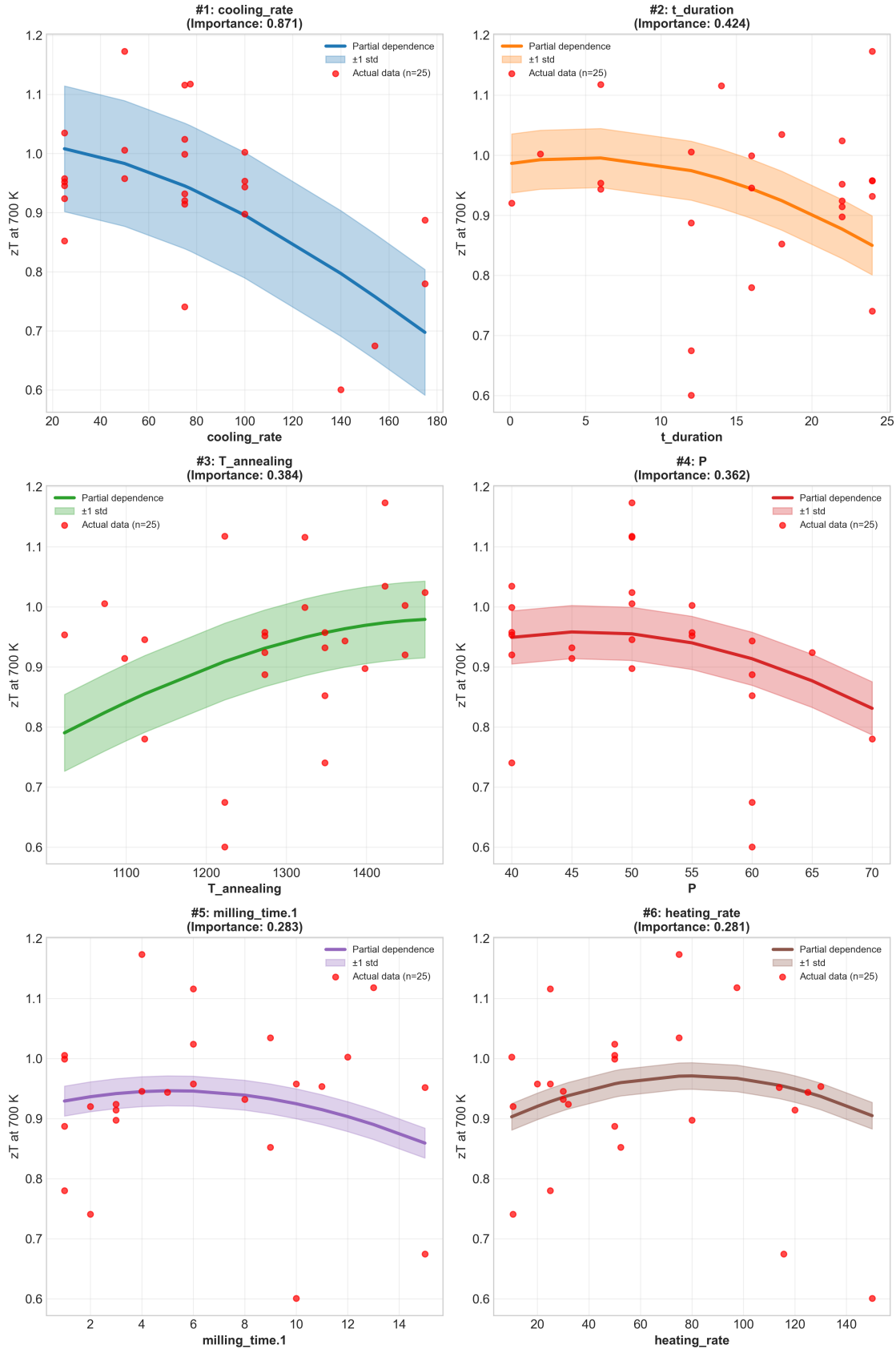


Figure S5: Partial dependence plots of the GP-fitted zT at 700 K for the six most important variables, in descending order: melt-cooling rate, dwell time, annealing temperature, SPS uniaxial pressure P , milling-time.1 and heating-rate. A ridge of high zT appears at rapid melt-quenching combined with short, slow-cooled SPS profiles.

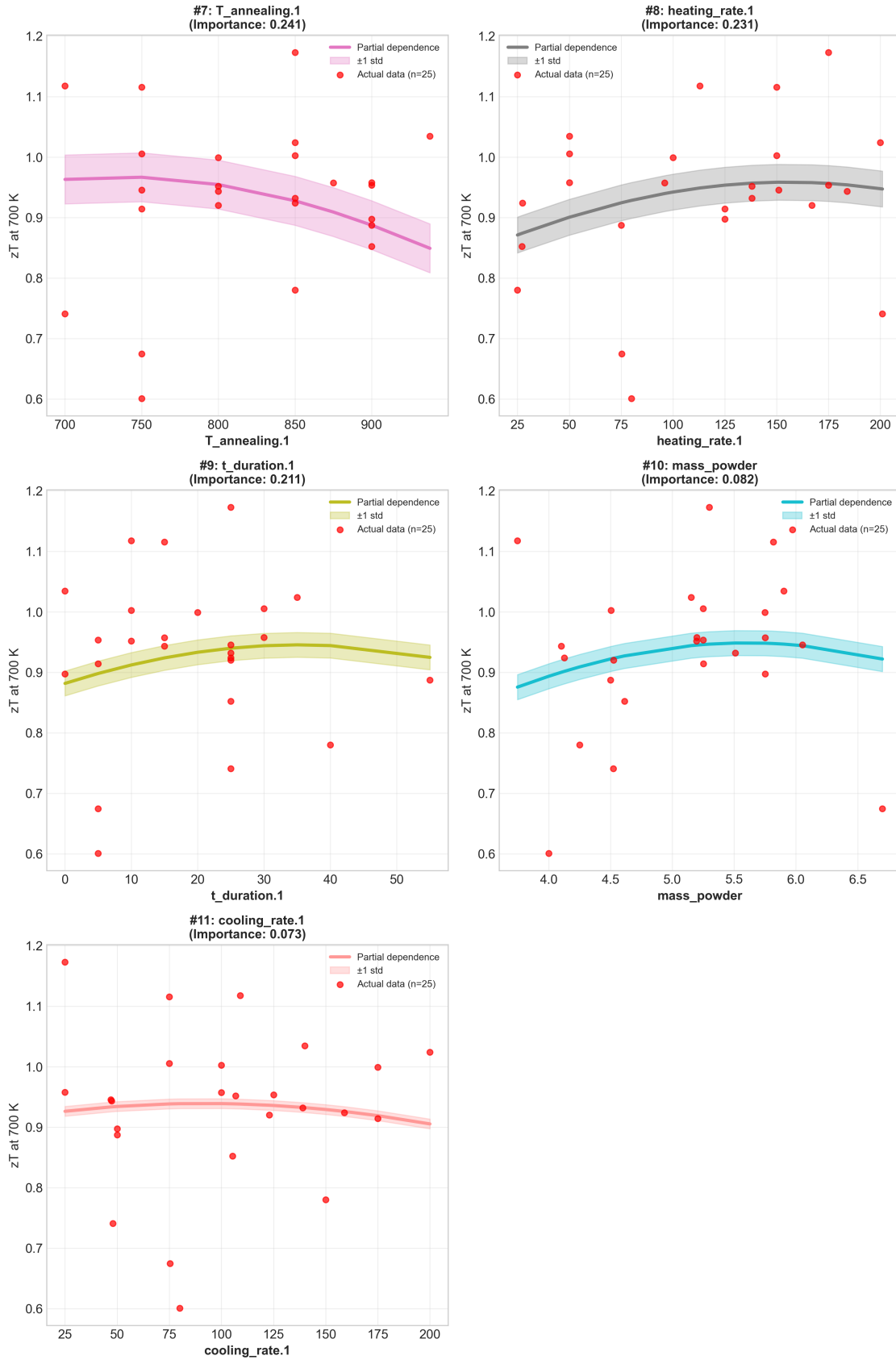


Figure S6: Partial dependence plots of the GP-fitted zT at 700 K for for the less influential variables, in descending order: annealing-temperature.1, heating-rate.1, dwell-time.1, mass-powder and cooling-rate.1. All show comparatively shallow trends, confirming their minor contribution to the overall variance in zT at 700 K.

References

- (1) Chattopadhyay, T.; Boucherle, J. X. Neutron diffraction study on the structural phase transition in GeTe. 1987; *J. Phys. C: Solid State Phys.* 20(10), 1431–1440. DOI:10.1088/0022-3719/20/10/012.
- (2) Li, J.; Chen, Z.; Zhang, X.; Sun, Y.; Yang, J.; Pei, Y. Electronic Origin of the High Thermoelectric Performance of GeTe among the *p*-Type Group IV Monotellurides. *NPG Asia Materials* **2017**, *9*, e353.
- (3) Chen, H.; Song, Q.; Zhang, Z.; Luo, T.; Wei, Q.; Sun, L.; Li, Y. Anisotropic Thermoelectric Properties of GeTe Single Crystals. *Journal of Materials Chemistry A* **2024**, *12*, 10974–10983.
- (4) Li, J.; Zhang, X.; Lin, S.; Chen, Z.; Li, W.; Pei, Y. Realizing the High Thermoelectric Performance of GeTe by Sb-Doping and Se-Alloying. *Chemistry of Materials* **2017**, *29*, 605–611.
- (5) Shuai, J.; Tan, X.; Guo, Q.; Zhang, Q.; Wang, H.; Pei, Y. Enhanced Thermoelectric Performance through Crystal Field Engineering in Transition-Metal-Doped GeTe. *Materials Today Physics* **9**, 100094.
- (6) Ding, G.; Gao, G.; Yao, K. High-efficient thermoelectric materials: The case of orthorhombic IV-VI compounds. 2015; *Sci. Rep.* 5:9567. DOI:10.1038/srep09567.
- (7) Allen, T.; Graser, J.; Issa, R.; Sparks, T. Machine learning predictions of low thermal conductivity: comparing TaVO₅ and GdTaO₄. 2023; ChemRxiv preprint. DOI:10.26434/chemrxiv-2023-444s3.
- (8) Armida, S. A.; Ebrahimibagha, D.; Ray, M.; Arenas, E.; Schaadt, K.; Treece, R. Assessing thermoelectric performance of quasi 0D carbon and polyaniline nanocomposites using machine learning. 2023; *Adv. Compos. Mater.* 33(3), 388–410.

- (9) Packwood, D. *Bayesian Optimization for Materials Science*; Springer: Singapore, 2017.
- (10) Lambard, G.; Sasaki, T. T.; Sodeyama, K.; Ohkubo, T.; Hono, K. Optimization of direct extrusion process for Nd-Fe-B magnets using active learning assisted by machine learning and Bayesian optimization. 2022; *Scr. Mater.* 209:114341. DOI:10.1016/j.scriptamat.2021.114341.
- (11) Gelbstein, Y.; Dado, B.; Ben-Yehuda, O.; Sadia, Y.; Dashevsky, Z.; Dariel, M. P. Highly Efficient Ge-Rich $\text{Ge}_x\text{Pb}_{1-x}\text{Te}$ Thermoelectric Alloys. *Journal of Electronic Materials* **2010**, *39*, 2049–2052.
- (12) Kumar, A.; Bhumla, P.; Parashchuk, T.; Arora, K.; Yadava, N.; Sachdev, K.; Bathula, S.; Tyagi, H.; Sharma, Y. Engineering Electronic Structure and Lattice Dynamics to Achieve Enhanced Thermoelectric Performance of Mn-Sb Co-Doped GeTe. *Chemistry of Materials* **2021**, *33*, 3611–3620.
- (13) Srinivasan, B.; Boussard-Plédel, C.; Bureau, B.; Le Gall, E.; Fan, X.; Halet, J.-F.; Halet, J.-F. Thermoelectric Performance of Codoped (Bi, In)-GeTe and (Ag, In, Sb)-SnTe Materials Processed by Spark Plasma Sintering. *Materials Letters* **2018**, *230*, 191–194.
- (14) Srinivasan, B.; Gellé, A.; Halet, J.-F.; Fan, X.; Boussard-Plédel, C.; Bureau, B. Detrimental Effects of Doping Al and Ba on the Thermoelectric Performance of GeTe. *Materials* **2018**, *11*, 2237.
- (15) Srinivasan, B.; Gellé, A.; Gucci, F.; Fan, X.; Boussard-Plédel, C.; Bureau, B.; Halet, J.-F. Realizing a Stable High Thermoelectric $zT \approx 2$ over a Broad Temperature Range in $\text{Ge}_{1-x-y}\text{Ga}_x\text{Sb}_y\text{Te}$ via Band Engineering and Hybrid Flash-SPS Processing. *Inorganic Chemistry Frontiers* **2019**, *6*, 63–73.
- (16) Srinivasan, B.; Le Tonquesse, S.; Gellé, A.; Fan, X.; Boussard-Plédel, C.; Bureau, B.; Halet, J.-F. Screening of Various Elements as Potential Effective Dopants for Ther-

- moelectric GeTe - An Experimental and Theoretical Appraisal. *Journal of Materials Chemistry A* **2020**, *8*, 19805–19821.
- (17) Perumal, S.; Samanta, M.; Ghosh, T.; Xie, L.; He, J.; Candidus, G.; Felser, C.; Biswas, K. Realization of High Thermoelectric Figure of Merit in GeTe by Complementary Bi and In Co-doping. *Joule* **2019**, *3*, 2565–2580.
- (18) Hong, M.; Chen, Z.; Yang, L.; Qin, J.; Zhang, T.; Hu, H.; Yang, J.; Li, J.-F. Realizing zT of 2.3 in Ge_{1-x-y}Sb_xIn_yTe via Reducing the Phase-Transition Temperature and Introducing Resonant Energy Doping. *Advanced Materials* **2018**, *30*, 1705942.
- (19) Hong, M.; Wang, Y.; Feng, T.; Liu, W.; Zhang, T.; Qin, J.; Yang, L.; Li, J.-F. Strong Phonon-Phonon Interactions Securing Extraordinary Thermoelectric Ge_{1-x}Sb_xTe with Zn-alloying-induced Band Alignment. *Journal of the American Chemical Society* **2019**, *141*, 1742–1748.
- (20) Hong, M.; Lyv, W.; Li, M.; Qin, J.; Zhang, T.; Hu, H.; Yang, L.; Li, J.-F. Rashba Effect Maximizes Thermoelectric Performance of GeTe Derivatives. *Joule* **2020**, *4*, 2030–2043.
- (21) Shuai, J.; Sun, Y.; Tan, X.; Guo, Q.; Wang, H.; Xie, H.; Snyder, G. J.; Pei, Y. Manipulating the Ge Vacancies and Ge Precipitates through Cr Doping for Realizing High-Performance GeTe Thermoelectric. *Small* **2020**, *16*, 1906921.
- (22) Liu, Z.; Gao, W.; Zhang, W.; Tan, X.; Wang, H.; Xie, H.; Zhang, Q.; Pei, Y. High Power Factor and Enhanced Thermoelectric Performance in Sc and Bi Co-doped GeTe: Hidden Role of Rhombohedral Distortion. *Advanced Energy Materials* **2020**, *10*, 2002588.
- (23) Xing, T.; Zhu, C.; Song, Q.; Wang, S.; Zhao, L.-D.; He, J. Realizing High-Efficiency Thermoelectricity in GeTe through Synergetic Band Engineering and Nanostructuring. *Advanced Materials* **2021**, *33*, 2008773.

- (24) Gao, W.; Liu, Z.; Zhang, W.; Tan, X.; Wang, H.; Xie, H.; Pei, Y. Improved Thermoelectric Performance of GeTe via Efficient Yttrium Doping. *Applied Physics Letters* **2021**, *118*, 033901.
- (25) Bourgès, C. M. C.; Lambard, G.; Sato, N.; Tachibana, M.; Ishii, S.; Mori, T. Process optimization on kesterite-based ceramics for enhancing their thermoelectric performances assisted by active machine learning approach. 2024; *Acta Mater.* *281*:120342. DOI:10.1016/j.actamat.2024.120342.
- (26) Roisnel, T.; Rodríguez-Carvajal, J. WinPLOTR: A Windows Tool for Powder Diffraction Pattern Analysis. 2001; *Mater. Sci. Forum* *378-381*, 118–123. DOI:10.4028/www.scientific.net/MSF.378-381.118.
- (27) Jones, D. R.; Schonlau, M. Efficient Global Optimization of Expensive Black-Box Functions. 1998; *J. Global Optim.* *13*(4), 455–492. DOI:10.1023/A:1008306431147.
- (28) The GPyOpt authors GPyOpt: A Bayesian Optimization framework in Python. 2016; Available at <http://github.com/SheffieldML/GPyOpt>.
- (29) Pedregosa, F. et al. Scikit-learn: Machine Learning in Python. 2011; *Journal of Machine Learning Research* *12*, 2825–2830.
- (30) Cheng, H.; Zhang, J.; Lin, C. Persistence of the R3m Phase in Powder GeTe at High Pressure and High Temperature. 2018; *J. Phys. Chem. C* *122*(50), 28460–28465. DOI:10.1021/acs.jpcc.8b06511.
- (31) Edwards, A. H.; Pineda, A. C.; Schultz, P. A. Theory of persistent, p-type, metallic conduction in c-GeTe. 2005; *J. Phys. Condens. Matter* *17*(32), L329–L335. DOI:10.1088/0953-8984/17/32/L01.
- (32) Alleno, E. et al. A round robin test of the uncertainty on the measurement of the ther-

- moelectric dimensionless figure of merit of $\text{Co}_{0.97}\text{Ni}_{0.03}\text{Sb}_3$. 2015; *Rev. Sci. Instrum.* **86**(1):011301. DOI:10.1063/1.4905250.
- (33) Nugraha, A. S.; Lambard, G.; Na, J.; Hossain, M. S. A.; Asahi, T.; Chaikit-
tisilp, W.; Yamauchi, Y. Mesoporous trimetallic PtPdAu alloy films toward enhanced
electrocatalytic activity in methanol oxidation: unexpected chemical compositions
discovered by Bayesian optimization. 2020; *J. Mater. Chem. A* **8**(27), 13532–13540.
DOI:10.1039/d0ta04096g.
- (34) Matsuda, S.; Lambard, G.; Sodeyama, K. Data-driven automated robotic experiments
accelerate discovery of multi-component electrolyte for rechargeable Li-O₂ batteries.
2022; *Cell Rep. Phys. Sci.* **3**(4):100832. DOI:10.1016/j.xcrp.2022.100832.
- (35) Gandhi, J. R.; Nehru, R.; Chen, S.-M.; Sankar, R.; Bayikadi, K. S.; Sureshkumar, P.;
Chen, K.-H.; Chen, L.-C. Influence of GeP precipitates on the thermoelectric properties
of P-type GeTe and $\text{Ge}_{0.9-x}\text{P}_x\text{Sb}_{0.1}\text{Te}$ compounds. *CrystEngComm* **2018**, *20*, 6449–
6457.
- (36) Xing, T.; Song, Q.; Qiu, P.; Zhang, Q.; Gu, M.; Xia, X.; Liao, J.; Shi, X.; Chen, L.
High efficiency GeTe-based materials and modules for thermoelectric power generation.
Energy & Environmental Science **2021**, *14*, 995–1003.
- (37) Tang, S.; Dresselhaus, M. S. Building the Principle of Thermoelectric *ZT* Enhancement.
arXiv:1406.1842, 2014.
- (38) Lookman, T.; Balachandran, P. V.; Xue, D.; Yuan, R. Active learning in materials
science with emphasis on adaptive sampling using uncertainties for targeted design. *npj*
Computational Materials **2019**, *5*, 21.
- (39) Zhang, H.; Xie, H. Spark-plasma sintering of thermoelectric materials: A review. *Small*
2021, *17*, 2006921.

- (40) Bochmann, S.; Schilm, J.; Gas, P.; et al. Round robin test of Seebeck and electrical resistivity measurements on CoSb_3 . *Journal of Electronic Materials* **2018**, *47*, 2534–2543.
- (41) Mockus, J.; Tiesis, V.; Zilinskas, A. In *Towards Global Optimisation 2*; Dixon, L. C. W., Szegő, G. P., Eds.; North-Holland: Amsterdam, 1978; pp 117–129.